Surface-Initiated Polymerization from Barium Titanate Nanoparticles for Hybrid Dielectric Capacitors

6 AUTHORS, INCLUDING:

Sergio Paniagua
Intel
17 PUBLICATIONS **555** CITATIONS

SEE PROFILE

Yun Sang Kim
University of Georgia
13 PUBLICATIONS **50** CITATIONS

SEE PROFILE

Joseph W. Perry
Georgia Institute of Technology
321 PUBLICATIONS **12,169** CITATIONS

SEE PROFILE

Seth Marder
Georgia Institute of Technology
669 PUBLICATIONS **26,765** CITATIONS

SEE PROFILE

# Surface-Initiated Polymerization from Barium Titanate Nanoparticles for Hybrid Dielectric Capacitors

Sergio A. Paniagua,[†,∥] Yunsang Kim,[‡] Katherine Henry,[†,⊥] Ritesh Kumar,[§] Joseph W. Perry,*[,†] and Seth R. Marder*[,†,‡]

[†]School of Chemistry and Biochemistry, [‡]School of Materials Science and Engineering, and [§]School of Chemical and Biomolecular Engineering, Georgia Institute of Technology, Atlanta, Georgia 30332, United States

S *Supporting Information*

ABSTRACT: A phosphonic acid is used as a surface initiator for the growth of polystyrene and polymethylmethacrylate (PMMA) from barium titanate (BTO) nanoparticles through atom transfer radical polymerization with activators regenerated by electron transfer. This results in the barium titanate cores embedded in the grafted polymer. The one-component system, PMMA-grafted-BTO, achieves a maximum extractable energy density of 2 J/cm³ at a field strength of ∼220 V/µm, which exhibits a 2-fold increase compared to that of the composite without covalent attachment or the neat polymer. Such materials have potential applications in hybrid capacitors due to the high permittivity of the nanoparticles and the high breakdown strength, mechanical flexibility, and ease of processability due to the organic polymer. The synthesis, processing, characterization, and testing of the materials in capacitors are discussed.

KEYWORDS: *phosphonic acid, barium titanate, nanocomposite, surface-initiated polymerization, dielectrics, capacitors*
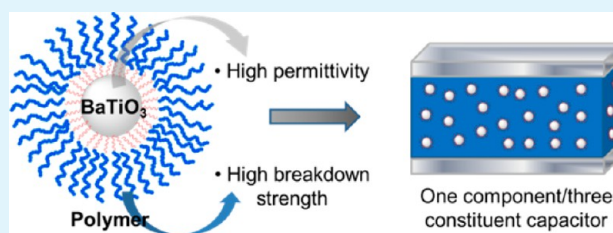
■ INTRODUCTION

The need for high-performance energy storage devices has served as motivation for the development of new materials for capacitors, super- and pseudocapacitors, batteries, and fuel cells.[1] Capacitors offer fast electrical charge and discharge responses; however, a compromise among weight, size, and energy density has to be achieved, so research is being done to miniaturize capacitors, reduce their weight per volume, and process them in new ways.[2] Metal oxides make up a commonly used class of dielectrics, often utilized for transistors and capacitors. Among these, BaTiO₃ (BTO) thin films with dielectric constants (ε_r) of ∼2500 can be obtained through a somewhat complex process involving chemical solution deposition followed by high-temperature sintering (900 °C) and reoxidation,[3] or via RF magnetron sputtering.[4] Nonetheless, the breakdown field is very low, and the processing conditions are often not compatible with flexible substrates. On the other hand, polymer-based insulators typically have good processability and high dielectric strengths but suffer from low permittivity, which limits their storage capacity.[5] For dielectrics in high-capacitance organic field-effect transistors (OFETs) and flexible capacitors, a hybrid approach combining inorganic oxides and organic materials could be suitable, as it can potentially take advantage of the high permittivity of the inorganic inclusions as well as the high breakdown strength, mechanical flexibility, and solution processability of the organic polymers.[5−9]

Capacitors based on BTO nanoparticles (which possess dielectric constants of up to ∼150 when bare) that have been surface-modified with phosphonic acids render the particle compatible with a host polymer, as we have previously explored.[5,10,11] The particles are then typically ball milled (mixed via grinding with the polymer for several days to make a dispersion) and spin coated onto a substrate, affording films with homogeneous nanoparticle dispersions. Promising devices have been obtained with this approach, with a relative permittivity (ε_r) of 37 ± 2 (at 1 kHz) for a 2,3,4,5,6-perfluorobenzyl phosphonic acid-modified BTO [50% (v/v)] and p(VDF-*co*-HFP), *aka* Viton [50% (v/v)] mixture, with a measured maximum energy density of up to 3.2 J/cm³ at a field strength of 164 V/µm.[11]

Nonetheless, there is still room for improvement in the breakdown field and energy storage, which can be achieved by preventing particle−particle contact and reducing voids. One potential approach to creating a high-performance polymeric−nanoparticle hybrid material would be to grow the polymer directly from the nanoparticles rather than using a two-component system. Such a system in which there was homogeneous growth of a polymer leading to a sufficient thickness to mitigate the propagation of breakdown paths has been shown to lead to enhancements in breakdown strength.[12] It also simplifies the material processing steps because there would be no compatibilization required with the polymer matrix as the polymer would be covalently attached to the nanoparticles, thus creating a one-component system with three constituents [the nanoparticles covalently attached to the
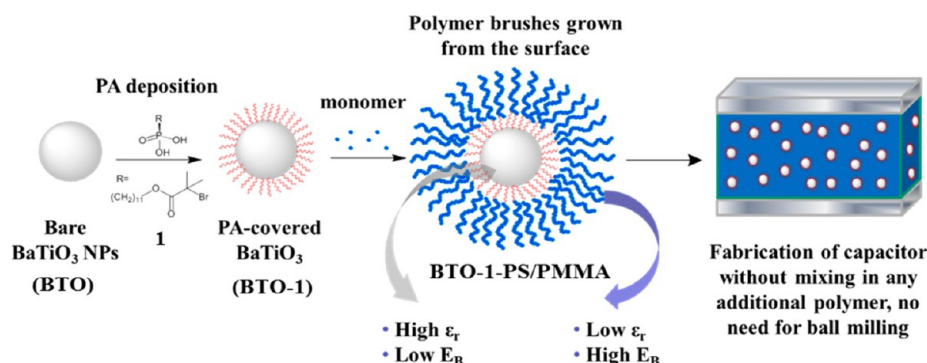
Figure 1. Scheme for creation of a one-component, three-constituent hybrid dielectric that can be used to build capacitors.

polymer via the phosphonic acid (Figure 1)]. Within the approaches for surface-initiated polymerization, atom transfer radical polymerization (ATRP) is currently one of the most widely used methods,[13] and there is an implementation of ATRP in which the activators are regenerated by electron transfer (ARGET ATRP),[14] which offers (a) continuous controlled polymerization, (b) constant regeneration of the Cu(I) activator by a reducing agent, (c) catalyst levels decreased to a level of parts per million from parts per thousand in regular ATRP, and (d) the opportunity to be done in the limited presence of air. These last two conditions make the application of this protocol simpler in practice than traditional ATRP because no further removal of copper is required and less stringent preparation conditions are used in ARGET ATRP.

Most surface-initiated polymerization studies from nanoparticles are reported using SiO_2 as the substrate; this is due to the widespread availability of commercial silica nanoparticles and synthetic methods for specific sizes and shapes.[15] Silane monolayers are typically used as initiators. However, SiO_2 has a low dielectric constant (3.9), making it unsuitable for high-ε_r dielectrics. Given that the surface chemistry is different for the titanates and the silicates,[16] the phosphonic acid functionality is used on the titanate. In this work, we report on the fabrication of a one-component, nanocomposite dielectric material consisting of BTO nanoparticles covalently attached to the nonconjugated polymer matrix. Detailed studies are presented on the surface-initiated polymerization from BTO and the morphological, dielectric, and energy storage characteristics of thin film capacitors fabricated from such nanocomposites.

RESULTS AND DISCUSSION

Modification of BTO with ATRP-Active PA. Phosphonic acid **1** was used in the procedure optimized by Kim[17] to modify commercially available barium titanate nanoparticles with an average size of 50 nm (see Experimental in the Supporting Information). In brief, the protocol consists of dispersing the nanoparticles via tip sonication in ethanol, adding the phosphonic acid, and refluxing the mixture at 80 °C overnight, followed by washing to remove noncovalently attached **1**. Scanning electron microscopy (SEM) images show no significant change in the particle morphology or size after the reaction (see Figure S1 of the Supporting Information). While there is some batch-to-batch variation in phosphonic acid coverage, it results in 60−130% of the expected monolayer, as the particles may have small variations in surface area that will affect the available surface area for reaction. IR spectra (Figure 2) show the absorptions seen in the free phosphonic acid with
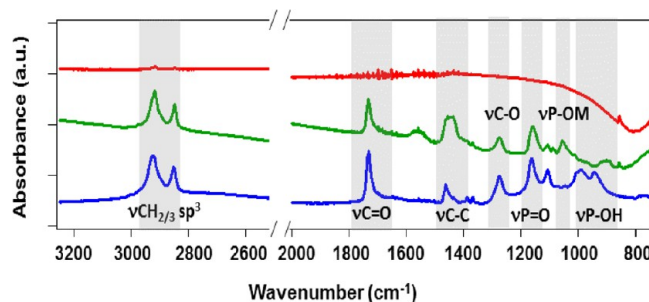

Figure 2. Comparison of IR spectra of the bare BTO (red), **1**-modified BTO (green), and phosphonic acid **1** (blue) in a KBr pellet.

some differences in the 1300−900 cm⁻¹ range: a new peak appears around 1050 cm⁻¹ (attributed to P−OM stretching),[4] while the broad peaks attributed to P−OH vibration disappear, and the P=O absorption is still observed. Magic angle solid state (MAS) nuclear magnetic resonance (NMR) showed that the ³¹P signal shifts and broadens upon attachment (see Figure S2 of the Supporting Information), which may be due to a mixture of bidentate and tridentate binding modes,[5] with P−OH groups no longer present.

ARGET ATRP Surface-Initiated Polymerizations. Polymerization via ARGET ATRP (Figure 3) was conducted by using a coper(II) complex that is reduced *in situ* using tin(II) ethylhexanoate as detailed in the Supporting Information. After the desired conversion percent is reached, the mixture is removed from the heat, opened to air, and precipitated into hexane to remove the monomer. The precipitate is then washed multiple times (at least three) with chloroform to remove any free polymer, reprecipitated, and dried under vacuum. The composites appear as a white powder, with no discernible green or blue color for Cu salts, as observed via conventional ATRP.

In this manner, material with a high organic content, of up to 57% residual mass as determined by thermogravimetric analysis (TGA), which translates into 37% polymer mass (see Table 1), is formed. The recovery is also very good in all cases (close to 0.5 g, having started with slightly <0.5 g of **BTO-1**) because there is no filtration involved, which is when most of the loss occurs in the case of conventional ATRP-produced composites. Table 1 summarizes some of the results. It is noticeable that increasing the temperature leads to a more grafted polymer, as does increasing the reaction time. The transmission electron microscopy (TEM) image of a composite with an intermediate polymer loading is shown in Figure 4a. Two control experiments were performed to verify that the polymerization was occurring from the monolayer of 2-bromo-2-methylpropi-
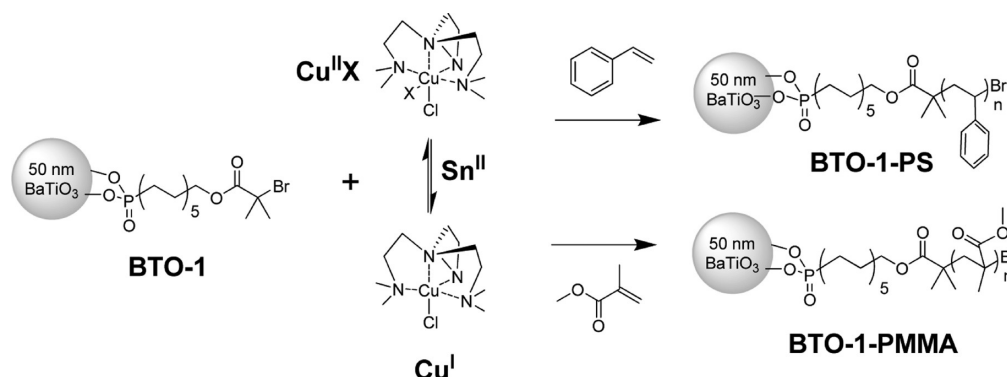
Figure 3. ARGET ATRP applied to surface-initiated polymerization of styrene or methylmethacrylate. A copper(II)-tris[2-(dimethylaminio)-ethyl]amine Cu^{II} is reduced *in situ* to the copper(I) complex Cu^{I}. This complex homolytically abstracts the halogen from the initiator, and the radical of **BTO-1** can undergo propagation with the monomer.

Table 1. Polymerization Conditions for the Synthesis of Polystyrene Composites

entry	St:BTO-1:Cu^I:Sn^{II}	time (h)	T (°C)	mass of polymer in composite (%)	BTO [% (v/v)]
1	400:1:0.04:0.2	7.5	90	7.6	49
2	400:1:0.02:0.2	3	110	13	39
3	340:1:0.02:0.2	6	110	22	29
4	400:1:0.03:0.2	16^a	105	25	27
5	600:1:0.06:0.3	20^a	110	37	19

^{a}Solidified overnight.

onate phosphonic acid on the nanoparticles through ATRP chemistry. (A) An inert PA such as octadecylphosphonic acid (OPA) was used to coat the BTO and attempt the polymerization in the same manner that was used for **BTO-1**, yielding no polymer attachment as shown in the Supporting Information, and (B) **BTO-1** was used without the addition of a copper salt or the reducing agent, resulting in a <1% increase in the organic content according to TGA, consistent with very a low polymerization efficiency.

Composites with Polymethylmethacrylate (PMMA). Given that films made with **BTO-1-PS** showed significant porosity (see Figure 4b) following our protocol for film deposition (see Experimental of the Supporting Information), composites with PMMA were prepared using the same protocol developed for PS, which resulted in more homogeneous films (*vide infra*). Conditions for surface-initiated polymerization of methylmethacrylate to create **BTO-1-**

PMMA composites, with varying polymer content, are summarized in Table 2. Higher polymer loadings are observed

Table 2. Results of Surface-Initiated Polymerization of MMA from ATRP PA-Modified BTO^a

	BTO-1-PMMA22	BTO-1-PMMA16	BTO-1-PMMA10
conditions	neat, 15 min	[M]/[A] = 1.0, 30 min	[M]/[A] = 3.8, 30 min
BTO [% (m/m)]	59.2	50.2	34.4
BTO [% (v/v)]	22	16	10
degraft M_n (kDa)	127	253	407
degraft PDI	1.6	1.7	2.2

^{a}[M]/[A] is the monomer to anisole concentration ratio.

than in the case of PS, with much shorter reaction times. As observed for the PS composites, increasing the concentration of the monomer leads to a higher polymer content. To better characterize the resulting composites, they were degrafted with acid treatments (see Figure S6 of the Supporting Information),[18,19] and the molecular weight distribution was measured by gel permeation chromatography (GPC). In general, as the polymer content increased, so did the molecular weight and the polydispersity index.

Capacitors Fabricated with the BTO-1-PMMA Composites. The composites were used to fabricate parallel plate
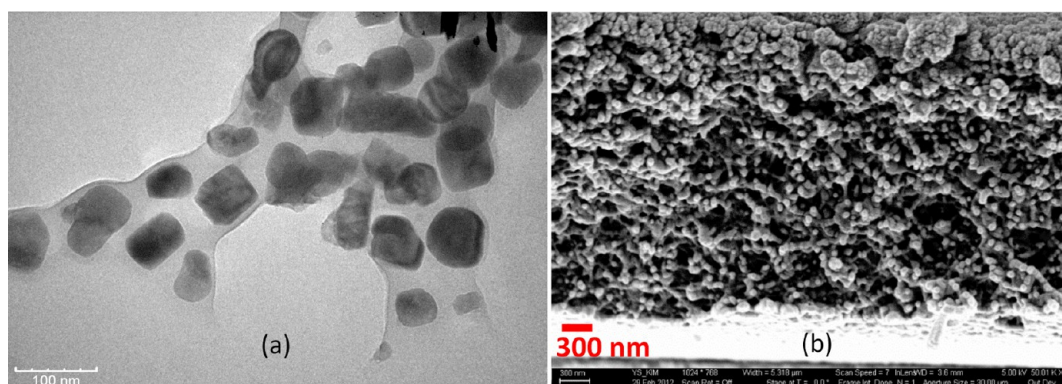
Figure 4. (a) TEM micrograph of **BTO-1-PS** composite 3 [29% (v/v) BTO] and (b) cross section SEM image for composite 5 [19% (v/v) BTO]. Scale bars are in nanometers.
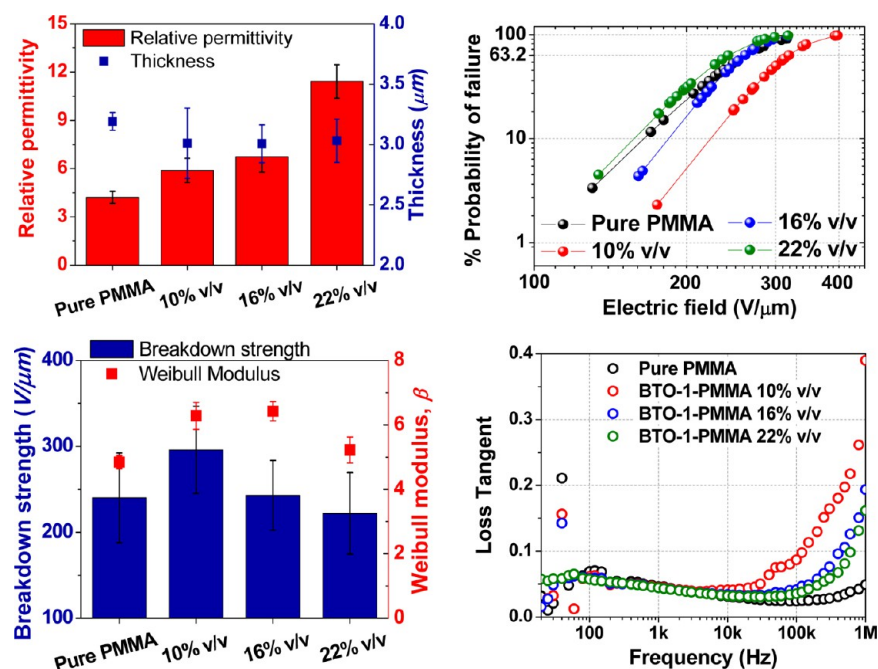
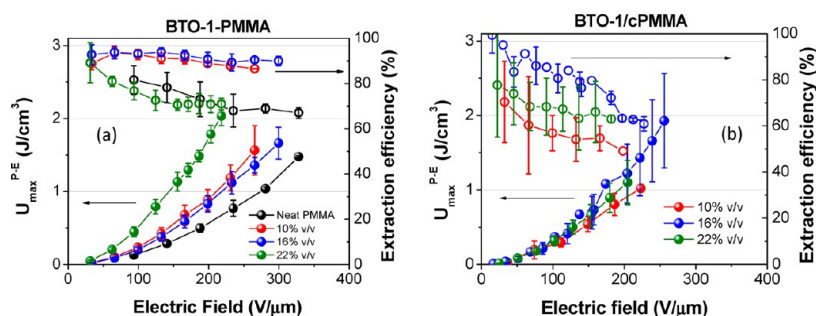**Figure 5.** Summary of device characterization of **BTO-1-PMMA** composites and pure PMMA.

Figure 6. Maximum energy density and extraction efficiency determined by $P-E$ of the devices made with the one-component dielectric (a) and the physical mixture of surface-modified BTO and PMMA (b).

capacitors as described in the Supporting Information. The films had similar thicknesses, ~3 μm, which made it possible for proper comparison of the breakdown strengths of nanocomposite films. The results are summarized in Figure 5. The permittivity increased as expected with a higher loading of BTO, reaching an ε_r of 11.4 for 22% (v/v) BTO (loadings of >30% resulted in permittivities of >13, but the breakdown strength was lower than 50 V/μm). For these grafted PMMA composites, the highest breakdown strength was for the 10% (v/v) BTO composite; pure homemade PMMA (M_n = 22 kDa; PDI = 1.3) showed breakdown strengths similar to those of the 16 and 22% (v/v) BTO composites. Breakdown analyses showed similar Weibull moduli for all composites. The energy storage characteristics of **BTO-1-PMMA** composites are presented in Figure 6a. The extractable energy density and extraction efficiency are determined from integration of the areas of the polarization–electric field ($P-E$) loops,[20] as shown in Figure S7 of the Supporting Information. The highest-loading composite [22% (v/v) BTO] gave the maximum extractable energy density (U_{max}) of 2 J/cm³, which can be attributed to the increased permittivity with little loss of breakdown strength compared to that of the lower-loading composites and neat PMMA.

Our results fare well upon being compared to the results of other efforts with composite dielectrics. Xie and co-workers[21] used an approach in which an ATRP-active silane modifier was synthesized in two steps from H_2O_2-treated 100 nm BTO, from which PMMA was grown. The highest permittivity reported, 15, was for a 20% (m/m) polymer, but neither breakdown fields nor maximum energy densities were reported. While the surface-initiated polymerization approach to covalent attachment usually results in high polymer loadings, the alternate *grafting to* approach is found more commonly in the literature given its simplicity, despite typically resulting in a low polymer coating and fewer customization possibilities if the work had already started with a premade polymer. Using the grafting to approach, Maliakal et al. prepared TiO_2 nanoparticle–PS composites, which suffered from a low dielectric constant (ε_r = 8) due to the use of TiO_2 instead of a higher-permittivity material and very low breakdown strengths (~2 V/μm).[22] Similarly, a permittivity of 6.4 (at 1 kHz) was reported by Tchoul et al., who used click chemistry to attach PS to TiO_2 nanorods.[23] State-of-the-art results for polymers attached to inorganics were reported by Jung and collaborators,[24] who recently reported dielectric constants as high as 45 (at 10 kHz) and a breakdown strength as high as 222 V/μm, resulting in calculated maximum energy densities close to the 10 J/cm³

D

benchmark (no measured maximum energy density was reported, which has been determined to be approximately 30−60% of the calculated value for a similar system[11]). They employed the grafting to approach as well, attaching polystyrene-b-poly(styrene-co-vinylbenzylchloride) to deprotonated BTO nanoparticles and reacting the resulting core−shell structure with triethylamine to convert residual vinylchloride groups to ammonium salts to increase the level of interaction with the oxide, stabilizing the polymer shell.

To determine the effect that covalent attachment of the polymer has on the dielectric properties of resultant nanocomposites, devices were fabricated to compare the one-component nanocomposites with those made by mixing the surface-modified nanoparticles with commercially available PMMA [cPMMA (Figure 7)]. Devices made by mixing

BTO-1

+

cPMMA
Mn = 52 kDa, PDI = 1.6

→ Mixed composite
BTO-1/cPMMA
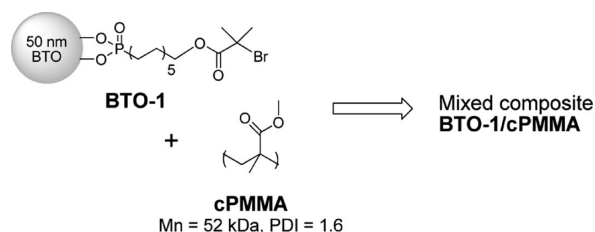
Figure 7. Physical mixture of ATRP-initiating phosphonic acid with commercial PMMA for device fabrication.

BTO-1 with cPMMA to afford 22% (v/v) BTO in the composite showed lower values for the benchmarks of the devices made with BTO-1-PMMA22: breakdown field of 205 V/μm versus a value of 218 V/μm [determined by $P-E$ loops (see the Supporting Information)] and an extraction efficiency of ∼60% (see Figure 7b) versus a value of ∼70% at ∼200 V/μm for the one-component dielectric, which resulted in a maximum extractable energy density of 1.1 J/cm^3, approximately half the value for the one-component system. It is noteworthy that SEM of the 22% (v/v) composite (BTO-1-PMMA22) in Figure 8a shows a uniform morphology with few pores, which contrasts with the microstructure of the BTO-1/cPMMA22 composite (Figure 8b). The improved morphology can be attributed to the covalent grafting of the polymer to the nanoparticles, which likely explains the improvement in the extractable energy density.

BTO-1/cPMMA16, which contains 16% (v/v) BTO mixed with PMMA, showed a U_{max} of 1.9 J/cm^3 at 256 V/μm (see Figure 6b). The one-component BTO-1-PMMA22 achieved a U_{max} of ∼2 J/cm^3 with a field 25% lower than that of BTO-1-/cPMMA16, which makes the simple mixture composite less energy efficient than the benchmark. Additionally, the energy density of BTO-1/cPMMA16 at ∼200 V/μm is only 1.2 J/cm^3, which is 40% lower than the U_{max} of the benchmark.

CONCLUSIONS

The ARGET ATRP methodology using surface-initiated polymerization from BaTiO$_3$ nanoparticles functionalized with a 2-bromo-2-methylpropionate-terminated phosphonic acid can be applied for the growth of nonconjugated polymers, needing fewer preparation procedures and less stringent purification steps than conventional ATRP. Longer polymerization times lead to higher polymer loadings in the composites. Higher polymer loadings correlated with higher molecular weights and broader weight distributions. Control experiments demonstrated the external initiation of the ARGET ATRP polymerization.

Capacitor results using one-component composites consisting of PMMA grown from the modified nanoparticles are reported. These composites resulted in higher maximum energy densities at lower fields compared to that of pure PMMA, especially for the highest nanoparticle loading presented; this can be attributed to the increased dielectric constant in the latter with a breakdown strength larger than or comparable to that of the pure polymer, and a homogeneous microstructure versus the simple mixing of the polymer with the modified nanoparticles. Optimization of film processing could afford even higher benchmarks for capacitors made through surface-initiated polymerization, and the synthetic procedure could be used for the incorporation of blocks with more polarizable groups such as acrylonitrile units, or growth of polymers from other perovskite nanoparticles and/or nanowires.

ASSOCIATED CONTENT

Ⓢ Supporting Information
Additional characterization of BTO-1 and composites, control experiments on surface-initiated ARGET ATRP using styrene as a test monomer, and experimental information about materials, synthesis, characterization, and device fabrication. This material is available free of charge via the Internet at http://pubs.acs.org.
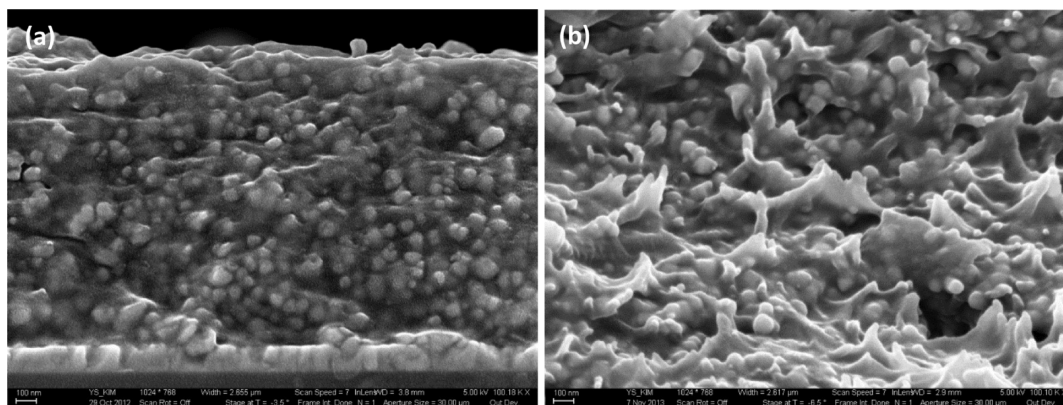
Figure 8. Cross sectional SEM for composites BTO-1-PMMA22 (a) and BTO-1/cPMMA22 (b), both 22% (v/v) in BTO. Scale bars are 100 nm. All samples were freeze-fractured in liquid nitrogen to minimize the structural change in the cross sectional samples.

■ AUTHOR INFORMATION

Corresponding Authors
*E-mail: joe.perry@gatech.edu.
*E-mail: seth.marder@chemistry.gatech.edu.

Present Addresses
∥S.A.P.: Portland Technology Development, Intel Corp., Hillsboro, OR 97124.
⊥K.H.: Department of Human Genetics, Emory University, Atlanta, GA 30322.

Author Contributions
S.A.P. and Y.K. contributed equally to this work.

Notes
The authors declare no competing financial interest.

■ REFERENCES

(1) Goodenough, J. B.; Abruna, H. D.; Buchanan, M. V. In *Basic Research Needs for Electrical Energy Storage. Report of the Basic Energy Sciences Workshop on Electrical Energy Storage*; April 2−4, 2007; DOE/SC/BES-0702; U.S. Department of Energy Office of Science: Washington, DC, 2007.

(2) Sarjeant, W. J.; Zirnheld, J.; MacDougall, F. W. *IEEE Trans. Plasma Sci.* **1998**, *26*, 1368−1392.

(3) Ilhefeld, J.; Laughlin, B.; Hunt-Lowery, A.; Borland, W.; Kingon, A.; Maria, J.-P. *J. Electroceram.* **2005**, *14*, 95−102.

(4) Schulmeyer, T.; Paniagua, S. A.; Veneman, P. A.; Jones, S. C.; Hotchkiss, P. J.; Mudalige, A.; Pemberton, J. E.; Marder, S. R.; Armstrong, N. R. *J. Mater. Chem.* **2007**, *17*, 4563−4570.

(5) Kim, P.; Jones, S. C.; Hotchkiss, P. J.; Haddock, J. N.; Kippelen, B.; Marder, S. R.; Perry, J. W. *Adv. Mater.* **2007**, *19*, 1001−1005.

(6) Li, J. Y.; Zhang, L.; Ducharme, S. *Appl. Phys. Lett.* **2007**, *90*, 132901.

(7) Smith, R. C.; Liang, C.; Landry, M.; Nelson, J. K.; Schadler, L. S. *IEEE Trans. Dielectr. Electr. Insul.* **2008**, *15*, 187−196.

(8) Ortiz, R. P.; Facchetti, A.; Marks, T. J. *Chem. Rev.* **2010**, *110*, 205−239.

(9) Tang, H.; Sodano, H. A. *Nano Lett.* **2013**, *13*, 1373−1379.

(10) Kim, P.; Zhang, X. H.; Domercq, B.; Jones, S. C.; Hotchkiss, P. J.; Marder, S. R.; Kippelen, B.; Perry, J. W. *Appl. Phys. Lett.* **2008**, *93*, 013302.

(11) Kim, P.; Doss, N. M.; Tillotson, J. P.; Hotchkiss, P. J.; Pan, M.-J.; Marder, S. R.; Li, J.; Calame, J. P.; Perry, J. W. *ACS Nano* **2009**, *3*, 2581−2592.

(12) Guo, N.; DiBenedetto, S. A.; Kwon, D.-K.; Wang, L.; Russell, M. T.; Lanagan, M. T.; Facchetti, A.; Marks, T. J. *J. Am. Chem. Soc.* **2007**, *129*, 766−767.

(13) Braunecker, W. A.; Matyjaszewski, K. *Prog. Polym. Sci.* **2007**, *32*, 93−146.

(14) Jakubowski, W.; Min, K.; Matyjaszewski, K. *Macromolecules* **2006**, *39*, 39−45.

(15) Radhakrishnan, B.; Ranjan, R.; Brittain, W. J. *Soft Matter* **2006**, *2*, 386−396.

(16) Mutin, P. H.; Guerrero, G.; Vioux, A. *J. Mater. Chem.* **2005**, *15*, 3761−3768.

(17) Kim, P. Surface Modification of Nanoparticles for Polymer/Ceramic Nanocomposites and their Applications. Ph.D. Thesis, Georgia Institute of Technology, Atlanta, 2008.

(18) von Werne, T.; Patten, T. E. *J. Am. Chem. Soc.* **2001**, *123*, 7497−7505.

(19) Babu, K.; Dhamodharan, R. *Nanoscale Res. Lett.* **2009**, *4*, 1090−1102.

(20) Kim, Y.; Kathaperumal, M.; Smith, O. N. L.; Pan, M.-J.; Cai, Y.; Sandhage, K. H.; Perry, J. W. *ACS Appl. Mater. Interfaces* **2013**, *5*, 1544−1547.

(21) Xie, L.; Huang, X.; Wu, C.; Jiang, P. *J. Mater. Chem.* **2011**, *21*, 5897−5906.

(22) Maliakal, A.; Katz, H.; Cotts, P. M.; Subramoney, S.; Mirau, P. *J. Am. Chem. Soc.* **2005**, *127*, 14655−14662.

(23) Tchoul, M. N.; Fillery, S. P.; Koerner, H.; Drummy, L. F.; Oyerokun, F. T.; Mirau, P. A.; Durstock, M. F.; Vaia, R. A. *Chem. Mater.* **2010**, *22*, 1749−1759.

(24) Jung, H. M.; Kang, J.-H.; Yang, S. Y.; Won, J. C.; Kim, Y. S. *Chem. Mater.* **2010**, *22*, 450−456.